Phase Control of Nonlinear Breit-Wheeler Pair Creation

Bernardo Maria Pereira da Costa de Pessanha Barbosa
bernardo.barbosa@tecnico.ulisboa.pt

Instituto Superior Técnico, Lisboa, Portugal

Month 2022

Abstract

Electron-positron plasmas are present in the vicinity of astrophysical objects, e.g. neutron stars. This is one of the reasons that contribute to general interest to investigate the behavior of these plasmas, which highly contrast regular laboratory ion-electron plasmas due to the symmetry of the species' mass. The laboratory production of electron-positron plasmas in enough amount to observe collective phenomena is a challenge in modern physics. One way to generate electron-positron pairs is to collide an intense laser pulse with a relativistic electron beam. This setup allows for the production of high-energy photons via nonlinear Compton scattering, which afterward decay into electron-positron pairs via nonlinear Breit-Wheeler pair creation. A setback in these experiments currently is that the number of generated positrons is very low, and background signals can interfere with the data collection (e.g. from bremsstrahlung photons decaying into pairs). In this work, a scheme utilizing a two-colored laser pulse is presented to achieve spatial separation of the produced pairs during the laser-beam interaction, and separate them from the original electron beam. A theoretical model is introduced to predict when charge momentum separation occurs in a plane wave as a function of the parameters of the two-colored pulse (most importantly, the laser phase) and Particle-in-Cell simulations demonstrate the effect leads to measurable observables for future experiments. Simulations with a finite spot size laser show the physical separation of the charges and the current produced by their motion, which can be controlled by varying the relative phase of the two laser modes.

Keywords: Plasma Physics; Pair Creation; Quantum Electrodynamics; Particle-in-Cell Codes; High-Intensity Lasers; Two-Colored Pulses

1. Introduction

With the recent developments in high-intensity laser facilities, it is possible to reach regimes where Quantum Electrodynamics (QED) effects become relevant in the interaction of a laser with a relativistic electron beam. These facilities, which can reach multi PW powers, are able to deliver intensities on the order of $10^{23} - 10^{24}$ W/cm^2 [1–3]. Plasmas composed of electrons and positrons created by QED processes are theorized to occur in the vicinity of very massive and compact objects, such as neutron stars. [4, 5] This turns our attention to trying to replicate at least some of the physics of these plasmas in a laboratory setup, using intense electric fields to replicate the regime where QED processes allow for the creation of a large number of positrons. Some of the schemes proposed for production of these plasmas include production in electron-laser scattering experiments [6, 7], where the high intensity electromagnetic field is provided by a focused laser, and which I focus on during this study; and the Bethe-Heitler process [8, 9], which is similar to electron-laser scattering, but uses the electric field of a nucleus of an atom with high atomic number. Trapping and accumulating positrons emitted from β^+ decay [10] is also a possibility, but with an added concern due to the annihilation of the positrons with electrons from normal matter. The predominant QED processes when using electron-laser scattering are: radiation reaction, which, given the very high accelerations felt by electrons and positrons in the oscillatory laser fields, results in a significant decrease of particle energy due to the radiated electromagnetic energy; nonlinear Compton scattering [11], where an electron or positron emits a high energy photon in the presence of an intense laser field, losing some of its own energy in the process; and nonlinear Breit-Wheeler pair creation [12], where an energetic photon, also in the presence of the strong laser fields, decays into an electron-positron pair. The sequential and repeated occurrence of these processes can result in a QED cascade. One of the current experimental goals in strong-field plasma QED is to cascade a sufficient number of particles to produce a pair plasma where collective phenomena are observable. Using an electron-laser collision for pair production has the setbacks that the peak intensity of a high intensity laser pulse is quite difficult to determine with precision [13], and that detecting the produced pairs is also a challenge, since the initial beam has electrons which can mix with the signal, which should (and sometimes can) be avoided [14]. There may also be some other QED processes producing leptons which turn the distinction of pairs produced via nonlinear Breit-Wheeler process more difficult, like pairs produced via Bethe-Heitler process occurring in the background, or by the direct trident process, where an electron immediately releases an electron-positron pair. [15]

In this thesis, I introduce a new scheme using a two-colored laser pulse for generating a bulk electric current during pair creation, which provides a macroscopic signature without the need for a high-density plasma. An analogous setup has been used to show that this current exists in the case of a two-colored laser ionizing atoms [16]. The reason why this system shows this behavior is because the probability of ionizing an atom grows as the intensity of the electric field grows, which favors particle birth in some phases of the pulse. For the pair creation case, the system also has a higher probability of generating pairs if the electric field is stronger, therefore, a net current should be possible to observe, similarly to the ionization case. However, unlike the ionization case, in a pair plasma, both species have the same mass, therefore, a drift can easily be imparted to both electrons and positrons in opposite directions. This separation of charges would allow us to see a macroscopic signature of pair plasma-laser interaction, without needing to generate a high-density plasma, as in other studies of pair plasma group behavior [17]. It may also allow for an easier detection of the pairs, since species propagate dominantly in opposite transverse directions.

Here I propose a scheme which utilizes a laser pulse and its second harmonic with an offset in phase, to obtain phase control over the direction of the emitted pairs. In Section 2, a theoretical approach is deduced to predict when charge separation occurs to pairs born via nonlinear Breit-Wheeler process in a two-colored laser pulse and show that the net separation of the charges is dependent on the phase difference between the pulses, just like the case for ionization in electron-ion plasmas [16], not only obtaining a macroscopic effect of the dynamics of an electron-positron plasma without the need to generate a dense plasma, but also creating an electron and positron beam with opposite asymptotic angles. The setup used to demonstrate this effect is sketched in figure 1. A relativistic electron beam (in blue) is sent to collide head-on against a laser pulse with two frequencies (represented by the red ellipsoid with another blue one inside it, however, this happens only for representation purposes, and not actually to represent that one pulse has a larger spot size than the other). In gray is represented the path the gaussian laser pulses follow as time evolves. First, when the electrons reach the vicinity of the laser pulse, some hard photons are emitted towards the center of the pulse due to nonlinear Compton scattering. Then, these photons decay into pairs according to the nonlinear Breit-Wheeler pair creation. The pairs then proceed to either drift in opposite directions or not according to the phase offset between the two laser waves.

The predictions made in Section 2 are supported by Particle-in-Cell (PIC) simulations run in the framework of OSIRIS [18] with an added Monte Carlo module for the QED processes [19, 20]. In Section 3 OSIRIS simulations for finite sized laser pulses show the effect of phase control in the movement of the leptons, and the overall charge separation and symmetric transverse motion of the electrons and positrons after the interaction.

2. Analytical Study of Electron-Seeded Pair Generation in Two-colored Pulses - Ideal Description (Plane Wave)

We consider, as shown in the setup in figure 1, that a relativistic electron beam collides with a two-colored laser pulse. In the present study, the high-intensity laser is composed by the sum of two waves, where the second is the second harmonic of the first. An expression for the electric field **E** is, therefore, for linearly polarized waves (assuming propagation along the z axis and polarization in the x axis)

$$\mathbf{E} = E_1 \cos(\phi)\mathbf{e}_x + E_2 \cos(2\phi + \theta)\mathbf{e}_x \;, \qquad (1)$$

where E_1 and E_2 are the amplitudes of the 1st and 2nd harmonic fields, respectively, ϕ is the phase of the wave given by $\phi = \omega_0 t - k_0 z$ with ω_0 the angular frequency and $k_0 = \omega_0/c$ the wavenumber of the first harmonic with c the speed of light in vacuum, θ is an offset phase between both harmonics and $\vec{e_x}$ is a unit vector pointing in the x direction. In this section, we consider both harmonics as plane waves, however, in the next section, simulations are performed with pulses with finite size and duration.

Since the motion of the electrons and positrons is relativistic, Newton's 2nd law must be solved for the relativistic motion of these particles under the Lorentz force. A correct description would require the addition of a radiation reaction force. However,

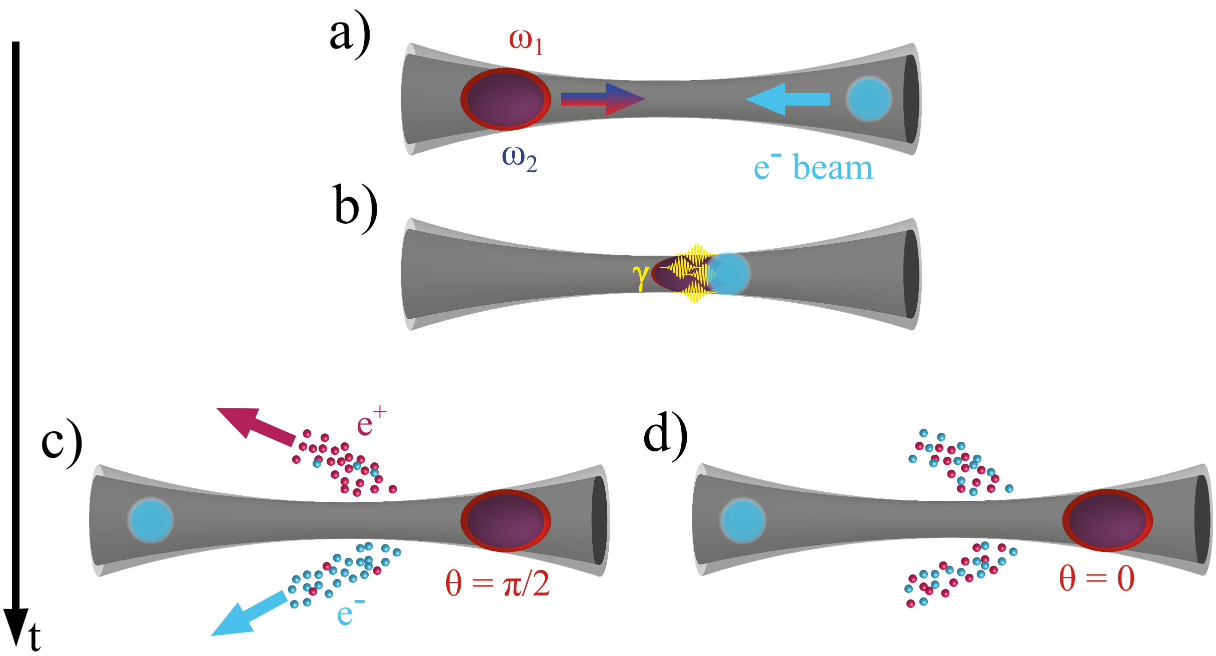

Figure 1: Schematic for a charge separation setup. a) an electron beam and two-colored laser pulse are sent in a head-on collision, b) the electrons emit photons due to nonlinear Compton scattering, c) for a phase offset θ of $\pi/2$ between the two colors of the pulse, the electrons and positrons tend to drift in opposite directions, d) for $\theta = 0$, this isn't observed, and each particle is equally likely to drift in any direction.

in this section, for simplicity, only the case of negligible radiation damping is discussed. Despite affecting the motion of the particles, the qualitative presence of a net current in the transverse direction shouldn't be altered, since radiation damping acts similarly to a drag force and wouldn't be able to swap the direction of drift of a particle. The equations of motion are then written as

$$\frac{d\gamma\beta_x}{dt} = \frac{qE_x}{mc}(1-\beta_z)\ , \tag{2a}$$

$$\frac{d\gamma\beta_y}{dt} = 0\ , \tag{2b}$$

$$\frac{d\gamma\beta_z}{dt} = \frac{qE_x}{mc}\beta_x\ , \tag{2c}$$

$$\frac{d\gamma}{dt} = \frac{qE_x}{mc}\beta_x\ , \tag{2d}$$

with $\boldsymbol{\beta} = \mathbf{v}/c$ with $\mathbf{v}$ the velocity of the particle, γ the Lorentz factor, m is the mass of the particle and q the charge of the particle. From the equations we have the conservation of two quantities

$$\gamma(1-\beta_z) = \text{const}\ , \tag{3a}$$

$$\gamma\beta_x + \frac{qA_x}{mc} = \text{const}\ , \tag{3b}$$

(3c)

with $\mathbf{A}$ being the vector potential satisfying $\mathbf{E} = -\partial\mathbf{A}/\partial t$ and here given by

$$\mathbf{A} = -\frac{E_1}{\omega_0}\sin(\phi)\mathbf{e}_x - \frac{E_2}{2\omega_0}\sin(2\phi+\theta)\mathbf{e}_x\ . \tag{4}$$

This alongside with the definition of Lorentz factor $\gamma = (1-\beta^2)^{-1/2}$ allows us to calculate the final velocity of a particle born somewhere along the pulse. This analysis is also valid for a pulse whose envelope varies very slowly in time, in comparison with the temporal variation associated to the oscillating fields. With this in mind, assuming pairs are born moving only in the z direction (the angle of emission will depend on $1/\gamma$, which for highly relativistic particles, allows us to neglect it) with velocity $v_{0z} = \beta_{0z}c$, the final drift velocity in the x direction is given by

$$v_{drift} = \frac{q}{|q|}\frac{2\gamma_0(1-\beta_{0z})a_1(\sin\phi_0 + \frac{E_2}{2E_1}\sin(2\phi_0+\theta))c}{1+\gamma_0^2(1-\beta_{0z})^2 + a_1^2(\sin\phi_0 + \frac{E_2}{2E_1}\sin(2\phi_0+\theta))^2}, \tag{5}$$

where ϕ_0 is the phase at which the particle is born and $a_1 = eE_1/mc\omega_0$. This velocity describes how fast the electrons and positrons drift in the polarization direction after they leave the pulse. It is important to highlight that v_{drift} has an opposite sign for positrons and electrons, which means that they drift at the same rate in opposite directions. The opposite-sign drift velocity could ultimately result in a spatial separation of the charges.

The electrons of the beam emit some photons via nonlinear Compton scattering, which then decay into pairs via nonlinear Breit-Wheeler pair creation, as illustrated in figure 1. These processes are governed by two quantum parameters η and χ, which are given by

$$\eta = \frac{\sqrt{|(F_{\mu\nu}p^{\mu})^2|}}{E_s m_e} \tag{6a}$$

$$\chi = \frac{\sqrt{|(F_{\mu\nu}\hbar k^{\mu})^2|}}{E_s m_e} , \tag{6b}$$

where $F_{\mu\nu}$ is the electromagnetic tensor, p^{μ} is the momentum 4-vector, $\hbar$ is the reduced Planck constant, $E_s = m_e^2 c^3/e\hbar$ is the Schwinger field [21] and k^{μ} is the wave 4-vector of the photon. Since the particles are highly relativistic, conservation of momentum dictates that in the photon emission, the particles emit the photons in the direction of motion. Also, the photons decay into an electron-positron pair, partitioning their momentum in two parts.

For a head-on collision along the z-axis, for the case of an electron or positron with Lorentz factor γ, the momentum four-vector is $p^{\mu} = (\gamma c, 0, 0, \gamma v_z)$ with $v_z < 0$. For the case of a photon with angular frequency ω, analogously, $k^{\mu} = (\omega/c, 0, 0, -\omega/c)$. With these 4-vectors, equations 6 can be simplified to

$$\eta = 2\,\frac{|E|}{E_s}\,\gamma , \tag{7a}$$

$$\chi = 2\,\frac{|E|}{E_s}\,\frac{\hbar\omega}{mc^2} . \tag{7b}$$

where $|E|$ is the instantaneous total electric field.

The electric field is modeled in equation 1. Therefore we can replace its expression to determine how η and χ depend on ϕ

$$\eta = 2\gamma \frac{|E_1 \cos(\phi) + E_2 \cos(2\phi + \theta)|}{E_s} , \tag{8a}$$

$$\chi = 2\frac{\hbar\omega}{mc^2} \frac{|E_1 \cos(\phi) + E_2 \cos(2\phi + \theta)|}{E_s} . \tag{8b}$$

Since we have an expression for χ, η and v_{drift} of the pairs being born, we can estimate the total current being produced by averaging the drift velocity of each particle with the Breit-Wheeler pair creation rate, which will determine in which phases it is most likely for a photon to decay into a pair, and ultimately give rise to an asymmetry in the drift of the species, turning the production of an accumulated current I_{acum} possible, and given by

$$I_{acum} = \frac{2q}{c} \int_0^{2\pi} \int_{\eta_{min}}^{\chi - \eta_{min}} v_{drift} \frac{dN_{nBW}}{dt d\eta} d\eta d\phi_0 , \tag{9}$$

with $dN_{nBW}/dtd\eta$ the Breit-Wheeler pair creation rate[11] and η_{min} is obtained setting γ to 1 in equation 8a. This quantity accounts not only for the fact that some phases produce a higher drift velocity, but also that there are some phases where pair creation is more likely, giving therefore an estimate of the current dependency on ϕ_0. It is worth mentioning that equation 9 has no information on the spectrum of photons, and assumes a mono-energetic photon bunch decaying into pairs. This is an approximation that should bear good results when considering the critical photon frequency ω_{crit}, which corresponds to the characteristic energy carried by each photon, and defined according to the condition

$$\int_0^{\omega_{crit}} \omega \frac{dN}{dE} d\omega = \frac{1}{2} \int_0^{\omega_{cutoff}} \omega \frac{dN}{dE} d\omega , \tag{10}$$

with dN/dE the energy distribution of the photon spectrum and ω_{cutoff} the maximum frequency that a photon can have (assuming it removes all the kinetic energy from a lepton). This quantity can be calculated numerically assuming we know the photon distribution.

In order to see if I_{acum} has the correct dependency in θ and E_2/E_1, equation 5 is benchmarked with quasi-1D simulations of plane waves colliding against a photon bunch with a quantum synchrothron energy distribution and constant density. The output if the simulations is then compared with the prediction of equation 5 of a mono-energetic photon bunch generating leptons with half their energy in figure 2.

It is possible to see that I_{acum} correctly predicts the behavior of the system in the plane wave approximation, specially considering values close to the critical frequency (which in this case was of 1.25 GeV). It is best to have a phase difference of $\pm\pi/2$ (in agreement with Ref. [16] for ionization) and fields with similar amplitude to maximize the transverse momentum, and consequently, the produced current from the electron-positron pairs. It should be noted that this conclusion is derived from phase-considerations in an idealized plane wave description. In the next chapter, I investigate diffraction-limited laser pulses, finite transversely and in time, and considering radiation reaction. This allows investigating if the momentum results in an observable transverse species separation in a realistic setup.

3. Phase Control and Charge Separation with a Finite Gaussian Laser Pulse, Including QED Radiation Reaction

OSIRIS is used to simulate a head-on collision between a two-colored laser pulse and an electron beam. For this study, I am using 2D PIC-QED sim-

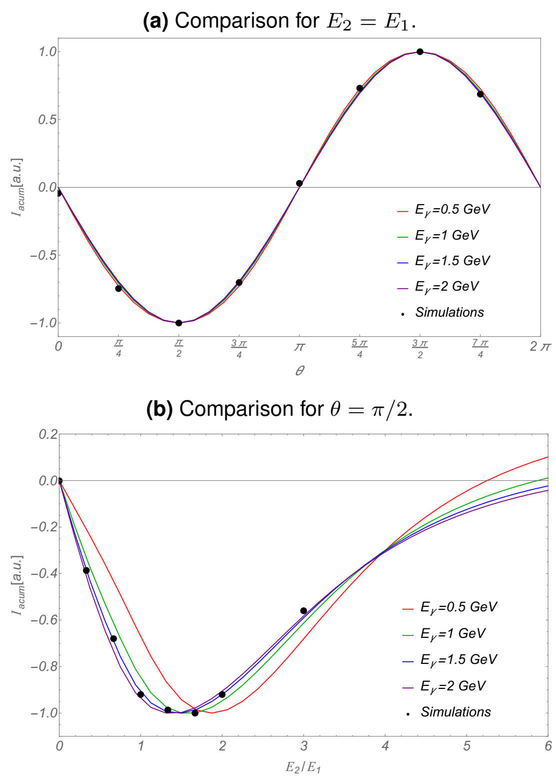

Figure 2: Comparison between the dependency in a) θ and b) E_2/E_1 of the produced current from theoretical predictions of various photon energies (in color) and simulations (black dots).

ulations. For the electron beam, I consider a monoenergetic beam with a gaussian density profile with the same standard deviation in all directions. The two-colored laser pulse is initialized by overlapping both laser frequencies using the same spot sizes. Since the pair production is linear with the number of electrons in the beam, one can extrapolate the total number of pairs or current generated for other electron beam charges. The laser focuses exactly when its center encounters the center of the electron beam. For this study, I ran 3 simulations for different values of θ, and for $E_2/E_1 = 1$. The simulation parameters can be found in table 1.

Variable	Value
ω_0	≈ 1.9 x10^{15} Hz
a_1	300
E_2/E_1	1
θ	$\pi/2$, $\pi/4$, 0
Laser duration	≈ 64 fs
Spot Size (both harmonics)	≈ 12.8 μm
Number of cells	8640 x 1800
Box size	≈ 70 x 80 μm
Δt	≈ 2.6 as
Particles per cell	2 x 2
e^- beam peak density	$\approx$ 10 pC/μm^3
e^- beam energy γ	≈ 5 GeV
e^- beam standard deviation	≈ 3.2 μm
e^- beam total charge	≈ 32 pC

Table 1: Simulation parameters for the simulations with finite spot size. Only θ was varied.

In order to visualize the charge separation of the electrons and positrons produced in the interaction, I present in figure 3 the their distributions for $\theta = 0$ and $\theta = \pi/2$ after ≈ 98 fs from the beginning of the simulation time. In the case where $\theta = 0$, the electrons and positrons drift both in positive and negative $x2$ direction, so despite having the drift of the particles, no charge separation is produced. However, for $\theta = \pi/2$ this is no longer true. Electrons have a preferential drift along the positive $x2$ direction while positrons show a preferential drift along the negative $x2$ direction. Due to radiation reaction, it is also observed that particles lose a large amount of their energy and begin co-propagating with the laser pulse (represented in purple).

The result of figure 3 achieves the main objective of this thesis: By controlling the phase offset θ between the two components of a two-colored laser pulse, it is possible to generate a current in the transverse direction and control the species separation among the generated electron-positron pairs. The fact that the laser eventually defocuses and liberates the particles that are co-moving with it ensures that, given enough time (which is computationally non-viable to simulate in the present runs) the product of the scattering will be two beams, one consisting mostly of electrons and another one of positrons, moving at opposite angles with relation to the optical axis.

Because both species get separated and move in opposite directions, $\theta = \pi/2$ is an ideal setup to maximize the produced current also in the finite-pulse scenario. A plot of the produced current both with $\theta = 0$ and $\theta = \pi/2$ is shown in figure 4. Here it is seen that the current deposited for $\theta = 0$ is barely distinguishable from noise, except in the region where particles are still oscillating under the influence of the pulse (where the current is produced by that oscillation, and not an overall drift). Meanwhile, for $\theta = \pi/2$ there are two large concentrations of current, both in the same direction but in opposite sides of the optical axis, due to both species moving in opposite directions and having opposite charges. A study is performed to understand where the net current is more intense and how it changes for the simulated values of θ. I define $I2_T$ as being the total current in a slice of constant $x2$, i.e

$$I2_T = \int_{x1_{min}}^{x1_{max}} J2 dx1 \; . \qquad (11)$$

This allows for the visualization of how close the

(a) Electron charge density for $\theta = 0$.

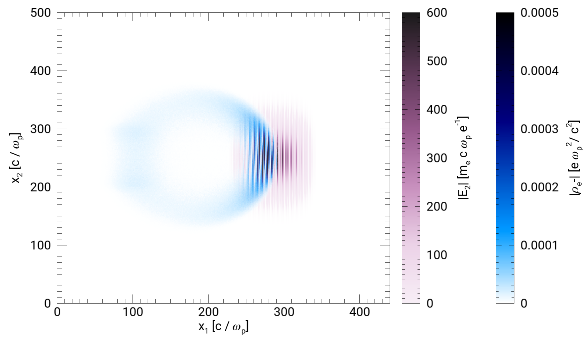

(b) Positron charge density for $\theta = 0$.

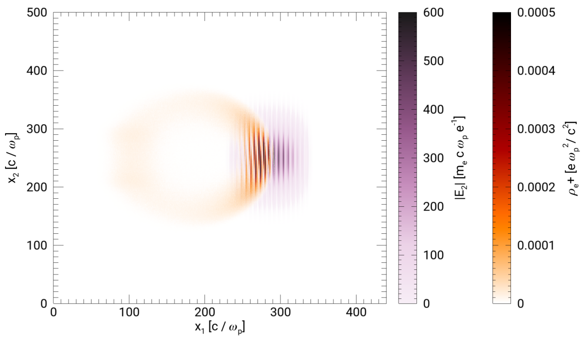

(c) Electron charge density for $\theta = \pi/2$.

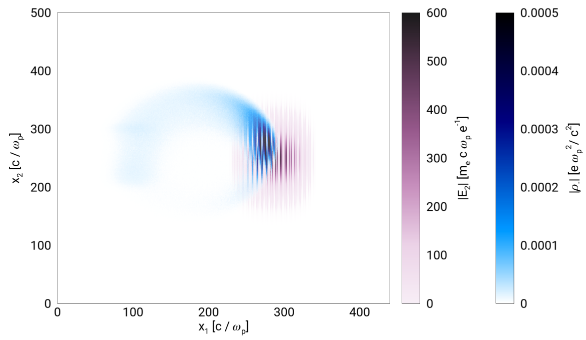

(d) Positron charge density for $\theta = \pi/2$.

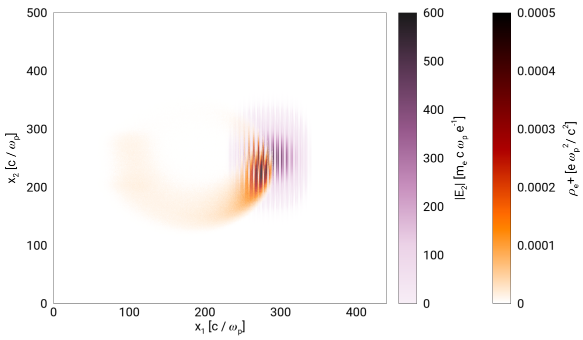

Figure 3: Charge density for electrons (in blue) and positrons (in red) for simulations with finite spot size with $\theta = 0$ (figures a) and b)) and $\theta = \pi/2$ (figures c) and d)).

maximum current is to the optical axis while neglecting the current produced by the particles oscillating in the laser fields (since that contribution averages to 0 in the integral), therefore I present a plot for this total current in figure 5a. From this plot, it is visible that the maximum of the current occurs around 30 μm and 50 μm, and that $\theta = \pi/2$ has a higher peak current than $\theta = \pi/4$, which agrees with the results from the previous section. Since the spot size of the laser is around 12.8 μm and the optical axis is located at $x2 = 40$ μm, I can conclude that most of the particles that contribute to the net current are nearly outside the most intense laser region. It is also visible that this plot is not perfectly symmetrical around the optical axis and that there is a small current for the case of $\theta = 0$. This small current changes sign around the optical axis and corresponds to a contribution of the ponderomotive force that the electrons in the beam feel when crossing the pulse. If I subtract this contribution to the remaining plots, symmetry around the optical axis is now observed in the currents produced as seen in figure 5b.

Finally, I investigate the impact that θ has on the number of pairs present in the simulation. A table with the ratio of the number of created pairs and initial electrons in the beam is found in table 2. From here, it is visible that the variation of θ keeps the variation in the number of pairs in the order of 2% and therefore don't contribute significantly to the increase of current observed.

θ	$N_{pairs}/N_{e}-$
0	6.0
$\pi/4$	6.1
$\pi/2$	6.1

Table 2: Ratio between number of pairs and initial number of electron for the values of θ simulated.

4. Conclusions

This thesis deals with phase control of species separation in Breit-Wheeler electron-positron beams. The pairs are generated from a head-on collision of electrons with a two-colored laser pulse. The two-colored laser can be experimentally obtained by overlapping a laser beam with its second harmonic.

I have derived an analytical model for the separation of electron-positron pairs born amidst a two-colored laser pulse. The theoretical analysis reveals that spatial separation of electrons and

(a) Transverse current density for $\theta = 0$.

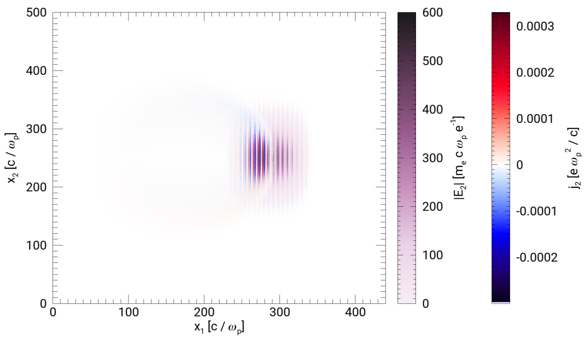

(b) Transverse current density for $\theta = \pi/2$.

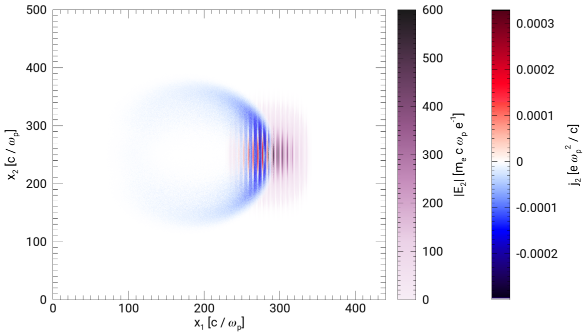

Figure 4: Transverse electric current generated by the movement of the produced pairs for a) $\theta = 0$ and b) $\theta = \pi/2$.

(a) Plot of $I2_T$ for $\theta = 0$, $\theta = \pi/4$ and $\theta = \pi/2$.

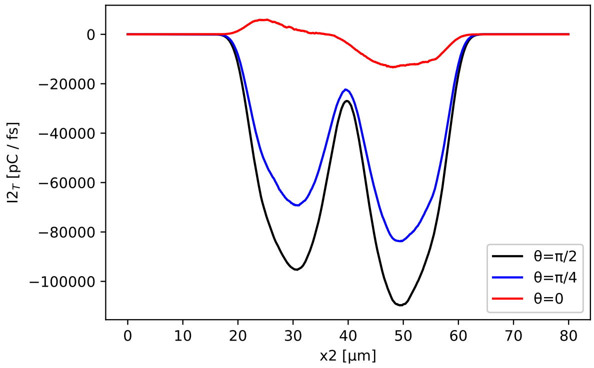

(b) Plot of $I2_T$ subtracting the contribution of $\theta = 0$.

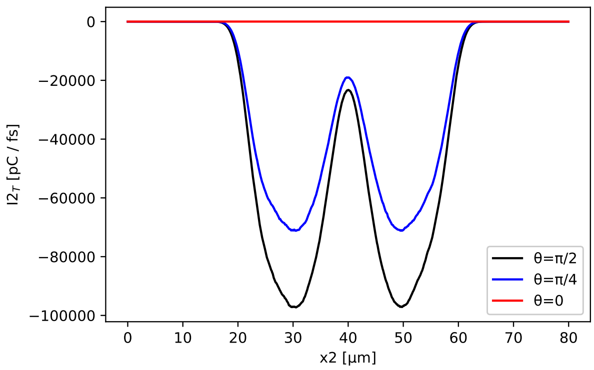

Figure 5: Plots of $I2_T$ vs. $x2$ for $\theta = 0$, $\theta = \pi/4$ and $\theta = \pi/2$. A moving average with 20 points has been done to smooth the plot.

positrons is directly related to the phase difference θ of the two laser modes, and by varying θ we can obtain a full separation or no separation at all. The phase scan can be used as a direct experimental signature of this effect.

The model assumes a transversely infinite plane wave for the laser beam. According to the analytical calculations, the optimal distribution of energy between the two harmonics is when the peak value of the electric field is comparable in each mode.

To confirm the validity of the theoretical description in non-ideal conditions, the same setup was studied with particle-in-cell simulations. The first verification was obtained using a plane wave with a finite envelope. This showed the same parametric dependencies as the model predicted. We then proceeded to full-scale, two-dimensional simulations, featuring a finite spot size, two-colored Gaussian laser pulse. Simulations of a head-on collision between a relativistic electron beam and this laser pulse were performed to further investigate the process of charge separation and show that the process could have macroscopic observable for laboratory experiments. We confirm that the maximum current generated by the particles being born via Breit-Wheeler pair creation in this setup occurs for phase differences of $\theta = \pm\pi/2$ and comparable values of the electric fields of each harmonic, just like the analytical estimates predict. This means that the effect is local, and the laser pulse transverse structure is not required to observe this process. For a single-mode laser (e.g. $E_1 = 0$ or $E_2 = 0$), the species separation is fully suppressed.

If the laser spot size is very small (of the order of the laser wavelength), it may happen that the ponderomotive force accelerates the charge separation once the leptons are first launched in opposite directions, and this could be a subject of a future investigation. Further work would include upgrading the theoretical model for it to predict the value of the obtained current density, instead of just identifying the optimal parameters where it is maximized. Computing the asymptotic angle of lepton escape in each direction would also be of interest to guide the detector design for experiments. A detailed study of emitted radiation from this system could reveal an additional experimental signature, analogously to the THz radiation emitted by a similar setup of two-colored laser ionization.

Original Contributions

The work which has lead to the completion of this thesis has led to contributions in the following peer reviewed papers:

- B. Barbosa et al, to be submitted to MRE (2022) : Analytical description and simulation confirmation of phase control of of charge separation in Breit-Wheeler pairs using two-color pulses;

- B. Martinez, B. Barbosa, M. Vranic, submitted, ArXiv https://arxiv.org/abs/2207.08728 : Calculations of low-energy pairs which are later used for plasma channel acceleration ;

- D. Ramsey et al, submitted (B. Barbosa in the Acknowledgments) : Enthusiastic discussions.

The work was presented at:

- PULSE Division Student Meeting, LLE, Rochester, June 2022;

- GoLP EPP Meeting, IST, November 2022.

Acknowledgments

I would like to thank my supervisors Marija Vranić and John Palastro for their guidance through all this work, Dillon Ramsey and Kathleen Weichman for all the help and feedback and Bertrand Martinez for many useful discussions. The work for this thesis has been funded by the project PTDC/FIS-PLA/3800/2021 and the computer simulations have been performed in: the Accelerates cluster, at IST; the MareNostrum cluster, based in the Barcelona Supercomputing Centre in Barcelona, Spain; and LUMI located in CSC's data center in Kajaani, Finland.

References

[1] S. Weber *et al.*, "P3: An installation for high-energy density plasma physics and ultra-high intensity laser–matter interaction at eli-beamlines," *Matter and Radiation at Extremes*, vol. 2, no. 4, pp. 149–176, 2017.

[2] B. Cros and et al., *Laser plasma acceleration of electrons with multi-pw laser beams in the frame of cilex*, 2014.

[3] *Exawatt center for extreme light studies*.

[4] P. Goldreich and W. H. Julian, "Pulsar Electrodynamics," *Astrophysical Journal*, vol. 157, p. 869, Aug. 1969.

[5] M. A. Ruderman and P. G. Sutherland, "Theory of pulsars: polar gaps, sparks, and coherent microwave radiation.," *Astrophysical Journal*, vol. 196, pp. 51–72, Feb. 1975.

[6] D. L. Burke *et al.*, "Positron production in multiphoton light-by-light scattering," *Phys. Rev. Lett.*, vol. 79, pp. 1626–1629, 9 Sep. 1997.

[7] M. Jirka, O. Klimo, M. Vranic, S. Weber, and G. Korn, "Qed cascade with 10 pw-class lasers," *Scientific Reports*, vol. 7, p. 15 302, Nov. 2017.

[8] H. Bethe and W. Heitler, "On the Stopping of Fast Particles and on the Creation of Positive Electrons," *Proceedings of the Royal Society of London Series A*, vol. 146, no. 856, pp. 83–112, Aug. 1934.

[9] B. Martinez, M. Lobet, R. Duclous, E. d'Humières, and L. Gremillet, "High-energy radiation and pair production by coulomb processes in particle-in-cell simulations," *Physics of Plasmas*, vol. 26, no. 10, p. 103 109, 2019.

[10] R. G. Greaves, M. D. Tinkle, and C. M. Surko, "Creation and uses of positron plasmas*," *Physics of Plasmas*, vol. 1, no. 5, pp. 1439–1446, 1994.

[11] N. P. Klepikov, "Emission of photons or electron-positron pairs in magnetic fields," *Zhur. Esptl. i Teoret. Fiz.*, vol. 26, 1954.

[12] G. Breit and J. A. Wheeler, "Collision of two light quanta," *Phys. Rev.*, vol. 46, pp. 1087–1091, 12 Dec. 1934.

[13] A. Galkin *et al.*, "Diagnostics of the peak laser intensity based on the measurement of energy spectra of electrons accelerated by the laser beam," *Proceedings of SPIE - The International Society for Optical Engineering*, vol. 7993, pp. 43–, Sep. 2010.

[14] M. Vranic, O. Klimo, G. Korn, and et al., "Multi-gev electron-positron beam generation from laser-electron scattering," *Sci Rep*, vol. 8, 2018.

[15] H. Hu, C. Müller, and C. H. Keitel, "Complete qed theory of multiphoton trident pair production in strong laser fields," *Phys. Rev. Lett.*, vol. 105, p. 080 401, 8 Aug. 2010.

[16] K. Kim, A. Taylor, J. Glownia, and G. Rodriguez, "Coherent control of terahertz supercontinuum generation in ultrafast laser–gas interactions," *Nature Photonics*, vol. 2, pp. 605–609, Jul. 2008.

[17] K. Qu, S. Meuren, and N. J. Fisch, "Signature of collective plasma effects in beam-driven qed cascades," *Phys. Rev. Lett.*, vol. 127, p. 095 001, 9 Aug. 2021.

[18] R. A. Fonseca *et al.*, "Osiris: A three-dimensional, fully relativistic particle in cell code for modeling plasma based accelerators," in *International Conference on Computational Science*, 2002.

[19] M. Vranic, T. Grismayer, J. L. Martins, R. A. Fonseca, and L. O. Silva, “Qed vs. classical radiation reaction in the transition regime,” *AIP Conference Proceedings*, vol. 1777, no. 1, p. 050 006, 2016.

[20] M. Vranic, “Extreme laser-matter interactions: Multi-scale pic modelling from the classical to the qed perspective,” Ph.D. dissertation, Instituto Superior Técnico, 2015.

[21] J. Schwinger, “On gauge invariance and vacuum polarization,” *Phys. Rev.*, vol. 82, pp. 664–679, 5 Jun. 1951.